Journal of Sol-Gel Science and Technology (2022) 104:464–469
https://doi.org/10.1007/s10971-022-05798-w

INVITED PAPER: FUNCTIONAL COATINGS, THIN FILMS AND MEMBRANES (INCLUDING DEPOSITION TECHNIQUES)

Preparation and gas barrier properties of cellulose nanocrystal-silica organic–inorganic hybrid gas barrier membranes with crosslinked structures

Koji Kuraoka [1,2] · Tomomi Iwasaki [1]

Received: 4 February 2022 / Accepted: 31 March 2022 / Published online: 23 April 2022

Abstract

Cellulose nanocrystal (CNC)-silica organic–inorganic hybrid gas barrier membranes were prepared by sol–gel method, and crosslinked structures of cellulose were introduced by crosslinking reaction using citric acid (CA). The effects of crosslinking agent (CA) content on the gas barrier property of the membranes were investigated. Water vapor transmission rate of C60 (60 wt% CA to CNC) was small (3.6 g m^{-2} day^{-1}), which is the same order of poly(vinylidene chloride) (PVDC). Oxygen permeability coefficients of C100 (100 wt% CA to CNC) was one-tenth of that of PVDC. Light transmittance of the organic–inorganic hybrid gas barrier membrane (C60) coated on the PET was 95%. And the pencil hardness of the membrane (C60) coated on the PET indicated HB. For the flexibility test, a 2 mm diameter stainless rod was attached to the membrane, and bent 10 times along the rod circle, no cracks were observed in the membrane surface. The hybrid gas barrier membranes exhibit higher oxygen and water vapor barrier properties with transparency, hardness and flexibility.

Graphical abstract

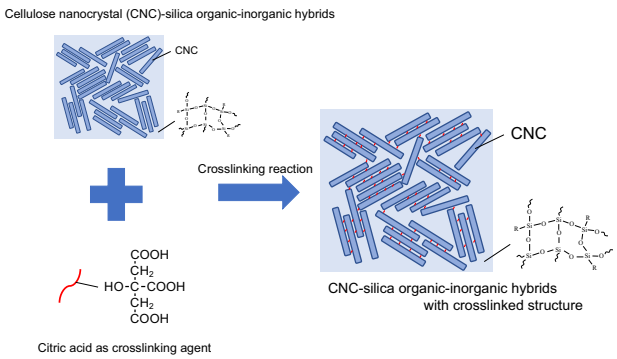

Keywords Cellulose nanocrystal · Silica · Organic–inorganic hybrid · Gas barrier membrane

✉ Koji Kuraoka
kuraoka@maritime.kobe-u.ac.jp

[1] Graduate School of Maritime Sciences, Kobe University, 5-1-1 Fukaeminami, Higashinada, Kobe 658-0022, Japan

[2] Research Center for Membrane and Film Technology, Kobe University, 1-1 Rokkodai, Nada, Kobe 657-8501, Japan

Highlights

- Cellulose nanocrystal (CNC)-silica organic–inorganic hybrid gas barrier membranes were prepared via sol–gel method, and crosslinked structures of cellulose were introduced by crosslinking reaction using citric acid (CA).
- The effects of crosslinking agent (CA) content on the gas barrier property of the membranes were investigated.
- C60 (60 wt% CA to CNC) exhibits the highest water vapor barrier property (water vapor transmission rate of 3.6 g m^{-2} day^{-1}).
- C100 (100 wt% CA to CNC) indicates the highest oxygen barrier property (oxygen permeability coefficients of 6.2×10^{-19} mol;m m^{-2} s^{-1} Pa^{-1}).

1 Introduction

The gas barrier membranes are mainly used as a packaging material in the food and medical fields for protecting products from oxygen and water vapor [1]. However, many of the widely used packaging materials are plastics derived from petroleum resources, and there are concerns about emission of greenhouse gases during incineration and plastic pollution in the ocean due to their non-biodegradability. Against this background, development of a gas barrier membrane using a natural polymer that can be decomposed by microorganisms, unlike plastics that are widely used, is expected from the viewpoint of environmental conservation. Therefore, the authors have focused on natural polymers such as polysaccharides (starch, chitin, chitosan, cellulose etc.), and has been researching and developing gas barrier membranes [2, 3]. Up to now, composites or hybrids have been produced by sol–gel method using silica as an inorganic component and cellulose as an organic component. In literatures, for example, cellulose/silica gel polymer hybrids were prepared by hydrolysis of acetyl cellulose in a sol–gel reaction [4], and cellulose/silica hybrid biomaterials were prepared by sol–gel covalent crosslinking process using tetraethoxysilane, γ-aminopropyltriethoxylsilane and 2,4,6-tri [(2-epihydrin-3-bimethyl-ammonium)propyl]-1,3,5-triazine chloride as crosslinking agent for improvement of thermal properties [5]. Although these papers are not on gas barrier membranes, organic–inorganic hybrid membranes are candidates for flexible and transparent high gas barrier materials and have been studied all over the world, such as silica/poly(vinyl alcohol) hybrid membranes prepared by sol–gel method [6, 7], silica/α-hydroxy polyethylene-block-poly (ethylene glycol) copolymers hybrid gas barrier membranes prepared by sol–gel method [8], polyvinylidene difluoride/silica hybrid gas barrier membranes prepared by atmospheric atomic layer deposition and electrohydrodynamic atomization [9], poly(methyl methacrylate)/silica hybrid gas barrier membranes prepared by sol–gel method [10]. However, there are no reports that have investigated the preparation and gas barrier properties of cellulose nanocrystal (CNC)-silica organic–inorganic hybrid gas barrier membranes.

In this paper, to improve the gas barrier properties, we investigated the introduction of silica network via sol–gel method and crosslinked structures of cellulose into the hybrid membranes at the nanometer level using a simple crosslinking agent (citric acid) to suppress the swelling of cellulose. Here we report the preparation and gas barrier properties of CNC-silica organic–inorganic hybrid gas barrier membranes with crosslinked structures.

2 Experimental

CNC-silica organic–inorganic hybrid gas barrier membranes were prepared via sol–gel method. Distilled water and CNC (crystal length: 100–200 nm, crystal diameter: 5–10 nm, crystallinity: ~100%) were stirred at room temperature for 1 day to prepare a 5 wt% CNC aqueous solution. The prepared solution was translucent and slightly opalescent. Nitric acid (HNO_3), methanol (MeOH), tetramethoxysilane (TMOS, $Si(OCH_3)_4$), 3-glycidoxypropyltrimethoxysilane (GPTMOS, $CH_2(O)CHCH_2OC_3H_6Si(OCH_3)_3$) were added into the solution, and the mixture was stirred at room temperature. A sol was prepared by adding citric acid (CA) as a crosslinking agent and further stirring at room temperature. Table 1 shows the compositions of the starting solution for preparing the membranes together with sample names. In Table 1, CNC content (wt%) is to alkoxide (TMOS + GPTMOS) weight and CA content (wt%) is to CNC weight. The prepared sol was spin-coated on polypropylene (PP) substrates for oxygen

Table 1 Sample name and the compositions of the starting solution for preparing the membranes (sol composition)

Sample	Sol composition (molar ratio)			CNC[a]	CA[b]
	TMOS	GPTMOS	HNO_3		
C0	0.7	0.3	0.03	50 wt%	0 wt%
C40					40 wt%
C60					60 wt%
C80					80 wt%
C100					100 wt%

[a]CNC content (wt%) is to alkoxide (TMOS + GPTMOS)

[b]CA content (wt%) is to CNC

permeation and polyethylene terephthalate (PET) substrates for water vapor permeation using a spin coater, and dried at 80 °C for 12 h to make a membrane.

Oxygen permeances through the membranes at 313 K were measured by a variable pressure method using a gas permeation measurement apparatus [6]. The membrane was placed in a temperature-controlled stainless steel membrane test cell, where the downstream volume and the upstream volume were well separated from each other. The measurement begins with the evacuation of the membrane test cell by the vacuum pump. After the evacuation, we supplied oxygen gas to the upstream volume at constant pressure and measured the increase in gas pressure in the downstream volume due to the gas permeation through the membrane. Gas pressure increase in downstream volume was recorded by time. Oxygen permeance was calculated from supplying gas pressure (pressure in the upstream volume), the downstream volume, the steady state time-dependent pressure change in the downstream volume and permeation area. And water vapor transmission rates (WVTR) of the prepared membranes were evaluated by dish method (JIS Z0208, ISO 2528) [6]. A test dish with a diameter of 60 mm and a depth of 25 mm was made from aluminum. Granular calcium chloride products were used to maintain the RH (relative humidity) inside the dish about zero. The membrane was cut into circle shapes and used to cover the test dish. The test dish with the membrane was kept in a chamber kept at 313 K and 90% in temperature and RH, respectively, and the weight of the dish was measured every 24 h. The WVTR was calculated from the weight change, elapsed time and permeation area. For multi-layer membranes, the following Eq. (1) was used for the permeability coefficient of the whole system (P) and the permeability coefficient of each layer (P_n).

$$\frac{L}{P} = \frac{L_1}{P_1} + \frac{L_2}{P_2} + \cdots + \frac{L_n}{P_n} \tag{1}$$

where L and L_n are the thickness of the whole system and each layer, respectively. Using this Eq. (1), the oxygen permeability coefficient of the organic–inorganic hybrid gas barrier membrane on PP substrate was calculated. And the WVTR of the membranes (normalized to 25 µm thickness) was also calculated by using Eq. (1), thickness is normalized as 25 µm [1].

X-ray diffraction (XRD) pattern of the membrane was recorded using an X-ray diffractometer (RINT2000, Rigaku Corp.) with an X-ray generator working at a power of 40 kV and 20 mA. The Cu Kα radiation was used to perform θ-2θ scans in an angular range from 10° to 60° with angle step size of 0.04°.

The pencil hardness test (load: 750 g) according to JIS K5600-5-4 (ISO 15184) was conducted to determine the surface hardness of the membrane coated on the PET substrate. For the flexibility test (cylindrical mandrel: JIS K5600-5-1, ISO 1519), a 2 mm diameter stainless rod was attached to the membrane, and bent 10 times along the rod circle, and then the membrane surface was observed with an optical microscope.

3 Results and discussion

WVTR of the membranes (normalized to 25 µm thickness) for CA content to CNC are shown in Fig. 1. WVTR of C0 (without CA) was 11.7 g m^{-2} day^{-1}. This value was much lower than that of cellulose film. The reported WVTR of microfibrillated cellulose and nanofibrillated cellulose films (normalized to 25 µm thickness) at 296 K 50% RH were 162–218 and 51–52 g m^{-2} day^{-1}, respectively [11]. The WVTR of C0 was about 5–18 times lower than those value. This higher water vapor barrier property is due to depress of cellulose swelling by rigid silica networks. WVTR of the membranes decreased to C60 (60 wt% CA to CNC) and then increased with the content of CA increased. The lowest value was 3.6 g m^{-2} day^{-1}. This value was about one-third of C0 (without CA). The decrease of WVTR is due to an increase in the crosslinking structure for CA addition. Further addition of CA caused the increase of WVTR due to an increase of hydroxyl (–OH) groups from CA. This is because –OH groups increase hydrophilicity of the membrane and promote swelling [12, 13].

Figure 2 shows oxygen permeability coefficients of the membranes for CA content to CNC. The oxygen permeability coefficient of C100 (100 wt% CA to CNC) was the lowest value, 6.2×10^{-19} mol m m^{-2} s^{-1} Pa^{-1}. The oxygen permeability coefficient of the membranes decreased to

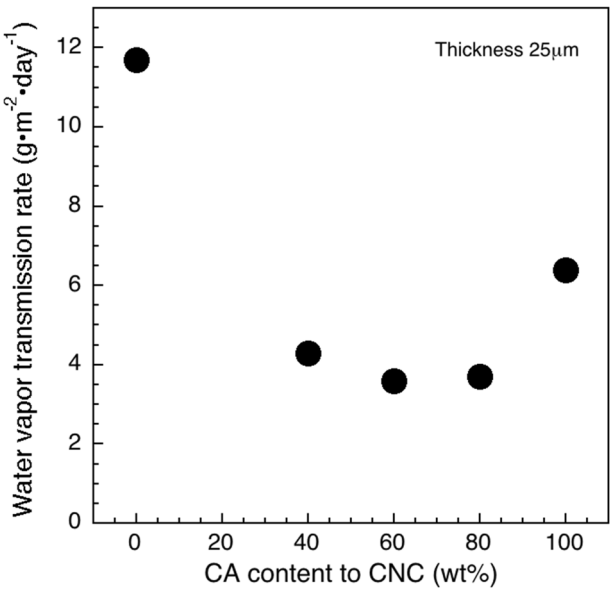

Fig. 1 WVTR of the membranes

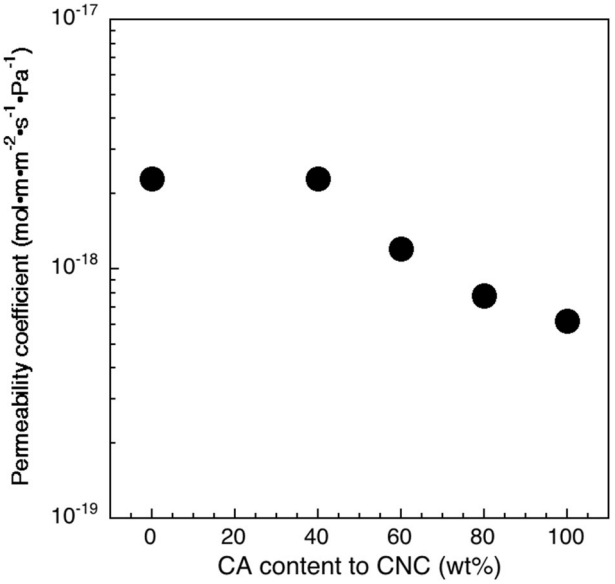

Fig. 2 Oxygen permeability coefficients of the membranes

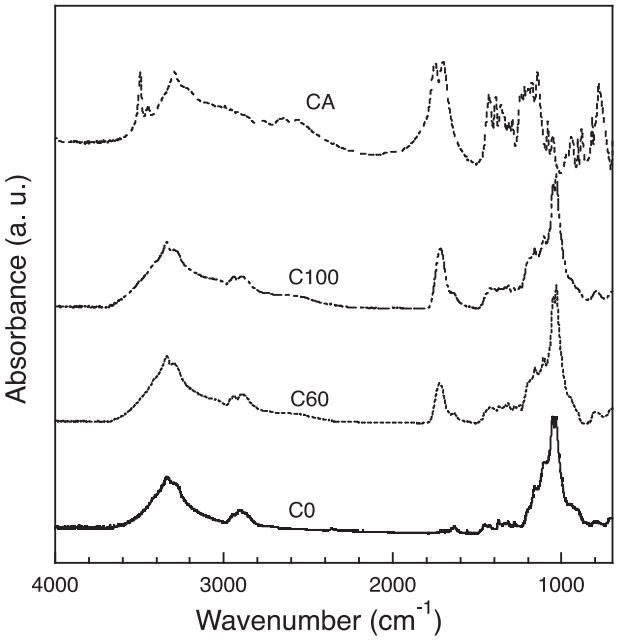

Fig. 3 IR spectra of C0, C60, C100, and CA from 4000 to 700 cm^{-1}

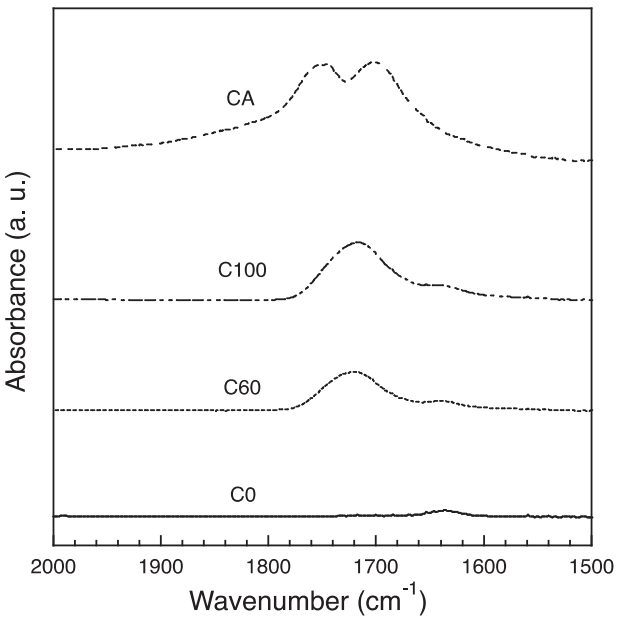

Fig. 4 IR spectra of C0, C60, C100, and CA from 2000 to 1500 cm^{-1}

C100 and then increased with the content of CA increased. The difference between the compositions showing the minimum values of oxygen permeability coefficient (C100) and WVTR (C60) is due to the fact that the oxygen permeation measurement is in a vacuum. This is probably because swelling does not occur in low humidity conditions, such as in a vacuum, and the structure becomes dense due to hydrogen bonds between –OH groups [12, 13].

The structures of the membranes were investigated by a Fourier transform infrared spectrometer (FT/IR-4100, JASCO Co.). The IR spectra of C0 (without CA), C60 (with the best water vapor barrier property), C100 (with the best oxygen barrier property) measured by ATR method and of CA measured by KBr method with simple transmission mode are presented in Figs. 3 and 4. Figure 3 shows the IR spectra from 4000 cm^{-1} to 700 cm^{-1}, and Fig. 4 shows the IR spectra from 2000 cm^{-1} to 1500 cm^{-1}. IR spectra of C0, C60 and C100 showed the characteristic bands related to Si–O–Si bond (~1220 and ~1080 cm^{-1}) [14, 15], which confirm the sol–gel reaction of TMOS and GPTMOS. Other characteristic bands originating from CA were also observed in Fig. 4. CA had two absorption peaks at around 1700 cm^{-1}. Some parts of CA are thought to exist as dimers with intermolecular hydrogen bonds between carboxyl groups [16]. Therefore, the absorption band of the monomer and the dimer C=O stretching vibration appears at ~1700 cm^{-1} [16, 17] and the absorption band of the dimer C=O stretching vibration appears at ~1750 cm^{-1} [16]. C0 (without CA) did not indicate such bonds, while C60 and C100 indicated one band at ~1720 cm^{-1}. The band at ~1720 cm^{-1} is the absorption band of C=O stretching vibration of ester bond due to esterification of carboxyl group in CA and hydroxyl group in CNC, and unreacted carboxyl group in CA [18, 19]. From the results, it was suggested that C60 and C100 had crosslinked structures of ester bonds formed by the reaction of carboxyl groups in CA and hydroxyl groups in CNC.

WVTR (normalized to 25 μm thickness) of C0, C60, C100, PVDC [20], PET [20] and PP [6] are shown in Fig. 5. WVTR of C60 was low, 1/5 that of PP, and showed the same order value as PVDC. C0 indicated not so high water vapor barrier property due to the structure without crosslinking.

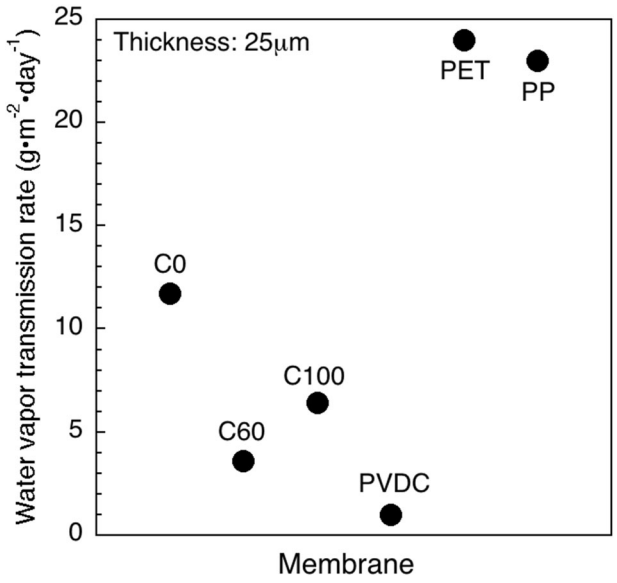

Fig. 5 WVTR of C0, C60, C100, PVDC, PET, and PP

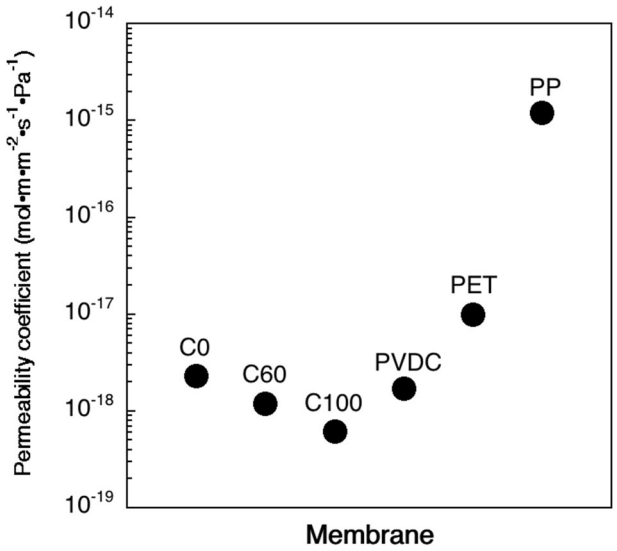

Fig. 6 Oxygen permeability coefficients of C0, C60, C100, PVDC, PET, and PP

And WVTR of C100 was not low due to swelling at high relative humidity (313 K 90%RH) with –OH groups.

Figure 6 shows oxygen permeability coefficients of C0, C60, C100, PVDC [20], PET [20] and PP [20]. The oxygen permeability coefficient of C100 was the lowest, 1/10 that of PVDC. The lowest value was due to many –OH groups in the membrane and the oxygen permeation measurement in vacuum.

The other properties of the prepared hybrid gas barrier membrane (C60) were evaluated. XRD pattern of C60 coated on a glass slide is shown in Fig. 7. The XRD pattern of the membrane consists of peaks assigned to (002) plane at ~23°, (101) plane at ~15° and (10$\bar{1}$) plane at ~17°

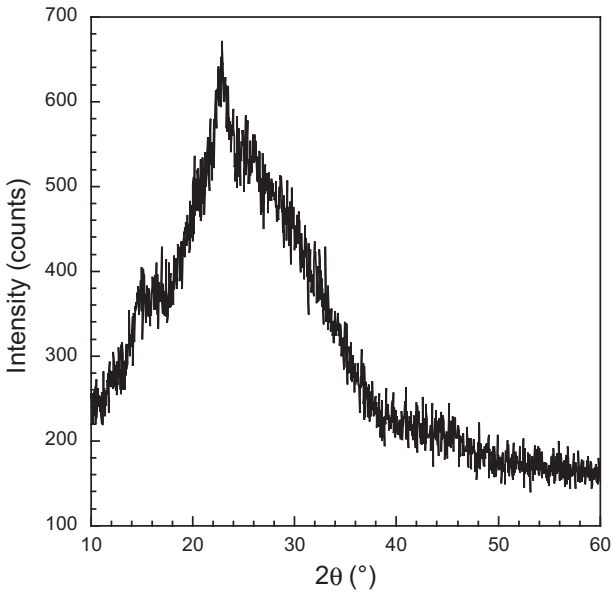

Fig. 7 X-ray diffraction pattern of C60 coated on a glass slide

[21, 22]. This result indicates the presence of CNCs in the membrane. The pencil hardness of the membrane indicated HB. This value was higher than that of the PET substrate (B) because calculated inorganic compound content in the membrane was 26.4 wt%. No cracks were observed in the membrane surface for the flexibility test. This result means that the prepared membrane is flexible, and the prepared organic–inorganic hybrid gas barrier membrane exhibits the flexibility with hardness due to the high dispersion of inorganic and organic components and the effect of SiO_2 networks. Light transmittance (wave length = 550 nm) was measured by ultra violet-visible spectrophotometer. Light transmittance of the organic–inorganic hybrid gas barrier membrane (C60) coated on the PET was 95% and higher than that of PET (Light transmittance = 90%) itself because the SiO_2 content in the membrane was high and the refractive index of the membrane was lower than PET. Therefore, it functioned like an antireflection film. This transparency is important for the practical applications of packaging and flexible electronics.

4 Conclusion

The CNC-silica organic–inorganic hybrid gas barrier membranes with crosslinked structures on plastic films were prepared by sol–gel method, and crosslinked structures of cellulose introduced by crosslinking reaction using CA. Oxygen permeances of the hybrid membranes were evaluated as the function of CA content. The oxygen permeability coefficient and the water WVTR (thickness 25 μm) were calculated from oxygen permeance and water WVTR

of the hybrid membrane and thickness of the membrane. The calculated values indicated that the hybrid barrier membranes obtained by sol–gel method and crosslinking reaction exhibits higher oxygen and water vapor barrier properties with transparency, hardness, and flexibility.

Author contributions All authors contributed to the study conception and design. Material preparation, data collection, and analysis were performed by KK and TI. The first draft of the manuscript was written by KK and all authors commented on previous versions of the manuscript. All authors read and approved the final manuscript.

Compliance with ethical standards

Conflict of interest The authors declare no competing interests.

Publisher's note Springer Nature remains neutral with regard to jurisdictional claims in published maps and institutional affiliations.

References

1. Kuraoka K, Shimmen Y, Kato H, Seki H, Nishikawa T (2020) Preparation and gas barrier properties of organic–inorganic hybrid gas barrier membranes using 3-glycidoxypropyl silsesquioxane. J Ceram Soc Jpn 128:229–232s
2. Kanazawa M, Kuraoka K (2013) Preparation of Silica/Starch Organic-inorganic Hybrid Gas Barrier Films with Cross-linked Structure -Effect of Addition of Tricarballylic Acid. J Packaging Sci Technol Jpn 22:347–356
3. Yamamoto R, Kuraoka K (2014) Preparation of Silica/Chitosan Organic-inorganic Hybrid Gas Barrier Membranes with Cross-linked Structure. J Packaging Sci Technol Jpn 23:435–442
4. Iwamura T, Akiyama K, Hakozaki T, Shino M, Adachi K (2017) Synthesis of cellulose/silica gel polymer hybrids via in-situ hydrolysis method. Polym Bull 74:4997–5009
5. Xie K, Yu Y, Shi Y (2009) Synthesis and characterization of cellulose/silica hybrid materials with chemical crosslinking. Carbohydr Polym. 78:799–805
6. Kuraoka K, Hashimoto A, Ashihara H (2010) Preparation and properties of silica/poly(vinyl alcohol) organic-inorganic hybrid gas barrier films via sol-gel method with microwave irradiation. Desalin Water Treat 17:66–71
7. Minelli M, De Angelis MG, Doghieri F, Rocchetti M, Montenero A (2010) Barrier properties of organic–inorganic hybrid coatings based on polyvinyl alcohol with improved water resistance. Polym Eng Sci 50:144–153
8. Minelli M, De Angelis MG, Doghieri F, Marini M, Toselli M, Pilati F (2008) Oxygen permeability of novel organic-inorganic coatings: I. Effects of organic-inorganic ratio and molecular weight of the organic component. Eur Polym J 44:2581–2588
9. Jagadeesan S, Lim JH, Choi KH, Doh YH (2018) Hybrid multi-layer thin-film fabrication by atmospheric deposition process for enhancing the barrier performance. J Coat Technol Res 15:1391–1399
10. Yeh J-M, Huang K-Y, Dai C-F, Chand BG, Weng C-J (2008) Organic-acid-catalyzed sol–gel route for preparing poly(methyl methacrylate)–silica hybrid materials. J Appl Polym Sci 110: 2108–2114
11. Kumar V, Bollstr"m R, Yang A, Chen Q, Chen G, Salminen P, Bousfield D, Toivakka M (2014) Comparison of nano- and microfibrillated cellulose films. Cellulose 21:3443–3456
12. Karlsson GE, Gedde UW, Hedenqvist MS (2004) Molecular dynamics simulation of oxygen diffusion in dry and water-containing poly(vinyl alcohol). Polymer 45:3893–3900
13. Nyflött Å, Meriçer Ç, Minelli M, Moons E, Järnström L, Lestelius M, Baschetti MG (2017) The influence of moisture content on the polymer structure of polyvinyl alcohol in dispersion barrier coatings and its effect on the mass transport of oxygen. J Coat Technol Res 14:1345–1355
14. Wong J, Angell CA (1976) Glass structure by spectroscopy. MARCEL DEKKER, INC., New York
15. Bertoluzza A, Fagnano C, Morelli MA, Gottardi V, Guglielmi M (1982) Raman and infrared spectra on silica gel evolving toward glass. Non-Cryst Solids 48:117–128
16. Bichara LC, Lanús HE, Ferrer EG, Gramajo MB, Brandán SA (2011) Vibrational Study and Force Field of the Citric Acid Dimer Based on the SQM Methodology. Adv Phys Chem 2011:1–10
17. Tarakeshwar P, Manogaran S (1994) Ground state vibrations of citric acid and the citrate trianion—an ab initio study. Acta A Mol Spectrosc 50:2327–2343
18. Yang CQ, Wang X, Kang I-S (1997) Ester Crosslinking of Cotton Fabric by Polymeric Carboxylic Acids and Citric Acid. Text Res J 67:334–342
19. Shi R, Zhang Z, Liu Q, Han Y, Zhang L, Chen D, Tian W (2007) Characterization of citric acid/glycerol co-plasticized thermoplastic starch prepared by melt blending. Carbohydr Polym 69:748–755
20. Kuraoka K, Miki K (2020) Gas barrier properties of inorganic–organic nanocomposite gas barrier membranes with high content of layered double hydroxide (LDH) using surface modified LDH. J Ceram Soc Jpn 128:573–576
21. Hamad WY, Hu TQ (2010) Structure–process–yield interrelations in nanocrystalline cellulose extraction. Can J Chem Eng 88:392–402
22. Xu X, Liu F, Jiang L, Zhu JY, Haagenson D, Wiesenborn DP (2013) Cellulose Nanocrystals vs. Cellulose Nanofibrils: A Comparative Study on Their Microstructures and Effects as Polymer Reinforcing Agents. ACS Appl Mater Interfaces 5:2999–3009